Range-dependent seabed characterization by inversion of acoustic data from a towed receiver array

Martin Siderius[a] and Peter L. Nielsen
SACLANT Undersea Research Centre, Viale San Bartolomeo 400, 19138 La Spezia, Italy

Peter Gerstoft
Marine Physical Laboratory, Scripps Institute of Oceanography, La Jolla, California 92093

(Received 2 April 2001; revised 31 January 2001; accepted 18 February 2002)

The MAPEX2000 experiments were conducted in the Mediterranean Sea in March, 2000 to determine seabed properties using a towed acoustic source and receiver array. Towed systems are advantageous because they are easy to deploy from a ship and the moving platform offers the possibility for estimating spatially variable (range-dependent) seabed properties. In this paper, seabed parameters are determined using a matched-field geoacoustic inversion approach with measured, towed array data. Previous research has successfully applied matched-field geoacoustic inversion techniques to measured acoustic data. However, in nearly all cases the inverted data were collected on moored, vertical receiver arrays. Results here show that seabed parameters can also be extracted by inverting acoustic measurements from a towed array of receivers, and these agree with those inverted using data received simultaneously on a vertical array. These findings imply that a practical technique could be developed to map range-dependent seabed parameters over large areas using a towed acoustic system. An example of such a range-dependent inversion is given using measurements from the MAPEX2000 experiments. [DOI: 10.1121/1.1502264]

PACS numbers: 43.60.Pt, 43.60.Gk, 43.30.Wi, 43.30.Xm [DLB]

I. INTRODUCTION

Sound propagation in shallow waters is known to vary drastically depending on location. Transmission-loss measurements taken around the world, in the frequency band of 0.5–1.5 kHz, show as much as 50 dB variability at 100-km source–receiver separations.[1] This variability can greatly influence the performance of a wide variety of sonar systems, and can be attributed to several environmental factors including surface wave-height conditions, water column sound-speed properties, bathymetry, and seabed type. The seabed often has a strong impact on propagation and its properties are probably the most difficult to obtain. Numerical models can be used to predict sonar system performance, but these rely on good information about the environment (e.g., seabed properties).

In recent years, model-based acoustic inversion techniques have been under development to determine properties of the seabed. Matched-field processing (MFP), geoacoustic inversion is a model-based technique that has been applied successfully in characterizing the seabed for the most important parameters for propagation prediction. This is a remote sensing method that uses down-range acoustic measurements to infer properties of the seabed. Computer simulations are used to model the down-range acoustic response to different seabed types, and efficient search algorithms are applied to find the environment giving an optimal match between modeled and measured data.[2–4] By far, the most common configuration has been a sound source and a vertical line array (VLA) of receivers spanning a large portion of the water column.[5–7] The VLA configuration is sensible as the propagating acoustic field is received at all angles (in the ideal case of $N\times 2D$ propagation with an array spanning the entire water column). In principle, if a towed sound source is used with a moored VLA, large areas could be probed and in some cases range-dependent seabed properties determined.[8] However, as the range increases between source and receiver, variability in the environment can destroy the prediction capability of the matched-field processor due to inaccuracies in the modeling. This variability could be caused by, among other factors, changes in bathymetry, variability in the ocean sound speed, or abrupt changes in the seabed properties. This range dependency can often be extremely difficult to include in the numerical modeling required for the MFP inversion, and may take some range-dependent propagation codes out of their region of numerical accuracy. While some factors like bathymetry might be well known and could be included in the MFP inversion modeling, other factors such as detailed, range-dependent, ocean sound-speed profiles are not likely to be available. For reliable seabed estimates, a geometry with either fixed source or receiver array may be limited to 2 km (or less) separation between the two due only the ocean sound-speed variability.[9] In addition, with either the source or receivers in a fixed location, the inverted bottom properties are averaged over the distance between the two. This is problematic in cases where distinct bottom types impact acoustic propagation in significantly different ways such that the behavior of the field would not be captured

[a]Currently at Science Applications International Corporation, 10260 Campus Point Dr., San Diego, CA 92121.

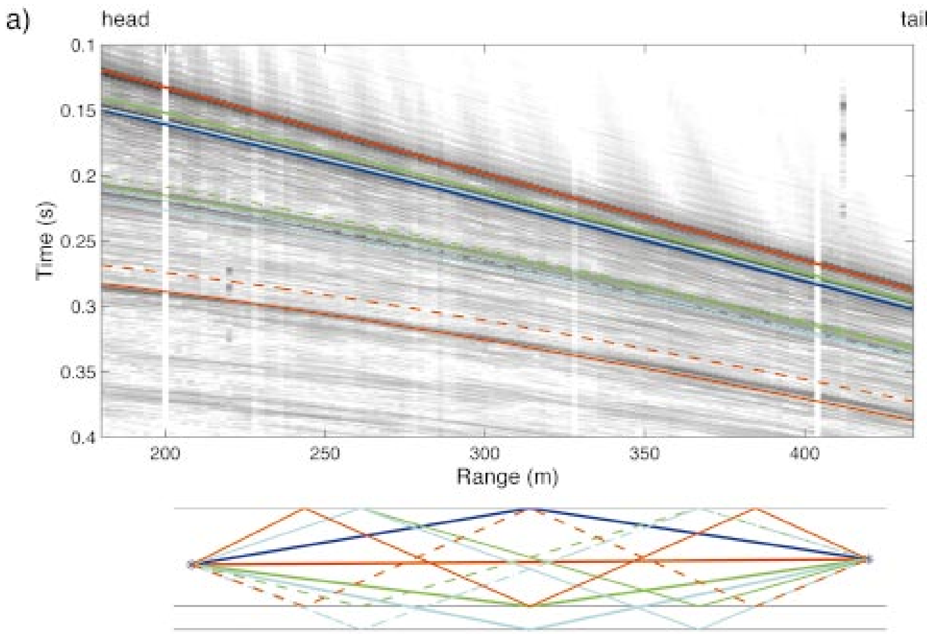

FIG. 1. Measured time series showing arrivals structure (top) and ray diagram to a single receiver (bottom). The ray diagram is based on simple geometric analysis and is color coded to help identify the corresponding arrivals on the measured time-series. The following geometry was used for the ray trace in bottom panel: source depth 72 m, head receiver depth 65 m, tail receiver depth 70 m, water depth 125 m sub-bottom depth 135 m, source-head receiver distance 180 m, and constant sound speed of 1510 m/s.

correctly using averaged seabed properties as input to a propagation model.

In this paper, matched-field geoacoustic inversion is considered using a towed horizontal line array (HLA). An HLA system has several advantages over a VLA including the ease in which it can be deployed from a ship. Since the HLA and towed sound source are kept at short range separations, MFP degradation due to water column sound-speed variability is minimized or eliminated. The requirement for range-dependent modeling in the MFP inversion is also eliminated because the bottom type and bathymetry can usually be assumed constant over the short distance separating source and HLA. Because of the short distance between source and HLA and because both are towed, distinct, range-dependent bottom types can be determined. A disadvantage of the HLA is that it does not span the water column and capture acoustic energy at all propagation angles. The inversion method described in this paper was motivated by the seismic industry where towed, horizontal arrays are commonly used. Examples of a seismic display using HLA measurements are shown in Figs. 1 and 2. In Fig. 1 the acquisition is for source and array at midwater depth with the head of the array about 180 m from the source. In Fig. 2, the source and array are closer to the sea surface. These figures indicate that the data contain information about a variety of propagation angles that have interacted with the bottom. The arrivals in Figs. 1 and 2—other than the direct and surface bounce—have information about the seabed sound speed, attenuation, and layer structure.

The seismic community has established techniques such as coring and wide-angle reflection measurements to determine seabed properties such as sound speed and density.

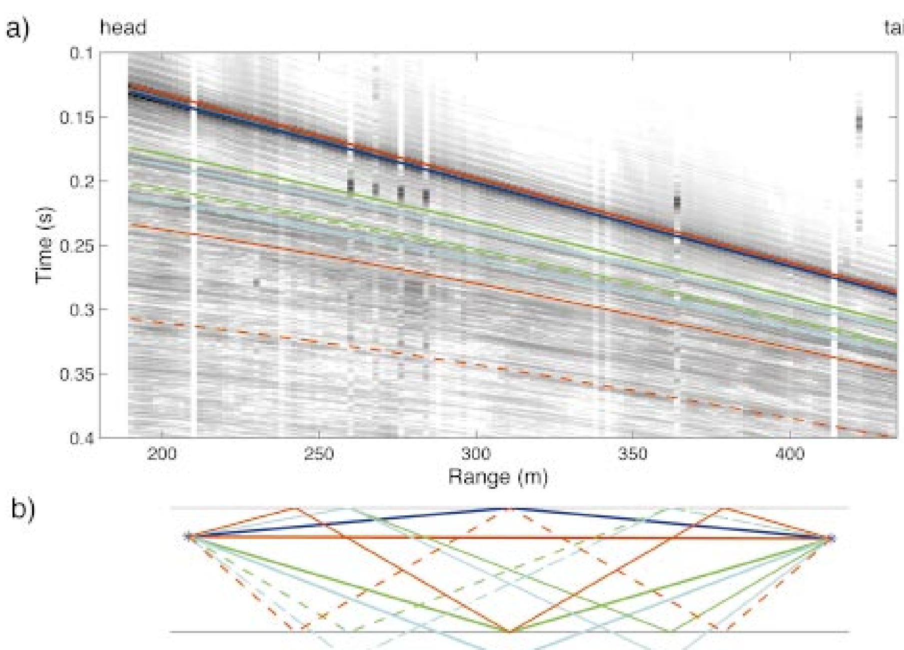

FIG. 2. Measured time series showing arrivals structure (top) and ray diagram to a single receiver (bottom). The ray diagram is based on simple geometric analysis and is color coded to help identify the corresponding arrivals on the measured time-series (bottom). There does not seem to be any arrivals corresponding to the bottom reflection (solid green) in the measured data. In the area for this data collection, the bottom is known to be soft and for shallow angles the reflection coefficient is close to zero. The following geometry was used for the ray trace in bottom panel: source depth 29 m, head receiver depth 30 m, tail receiver depth 31 m, water depth 121 m sub-bottom depth 130 m, source-head receiver distance 185 m, and constant sound speed of 1510 m/s.

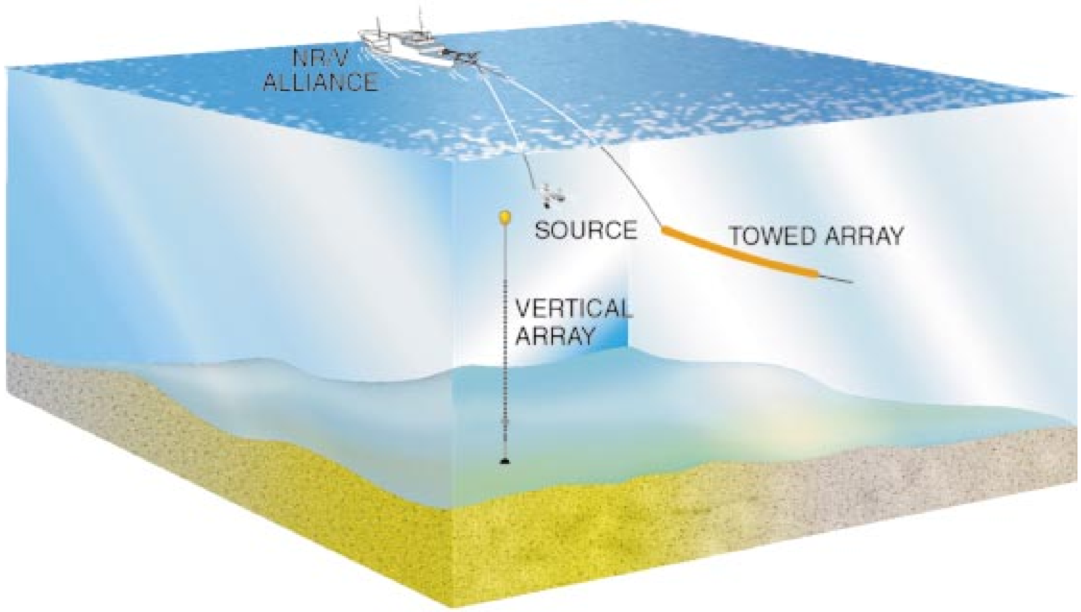

FIG. 3. Experimental geometry for 7 March 2000.

Coring methods are probably the most direct—this attempts to take a pristine sample of the seabed which is then analyzed (i.e., material sound speed is estimated by acoustic travel time measurements through the core). There are several drawbacks to coring as a way to produce quantities for input into numerical propagation models. Coring can typically only sample the top 1–5 m of the seabed. Harder seabeds (including sand) are often difficult (or impossible) to core. Coring is time consuming, requires specialized equipment not available on all ships, and is difficult in high sea states. Wide-angle reflection is another approach for estimating seabed properties. This acoustic technique estimates seabed layer thicknesses and sound speed by taking travel time measurements at different angles from the same reflector (same layer) in the seabed. Recently, using a moored receiver and towed sound source, this method has been extended to include the seabed loss parameter by also measuring seabed, frequency-domain bottom loss.[10] Although VLA, MFP geoacoustic inversions, can be problematic (for practical reasons and in range-dependent environments), this configuration has produced good simulated and experimental results. In particular, when source–receiver separations are small, or the range dependence weak, the VLA geoacoustic inversion can provide excellent seabed parameter estimates. In this paper, a VLA is used on conjunction with a towed HLA as shown in Fig. 3. Although the interest here is to develop a seabed characterization methodology based on an HLA, the VLA is used for comparing inverted seabed parameter estimates. It is important to show consistency between these two configurations as the VLA inversion is probably closest to ''ground-truth'' knowledge of the seabed available. To insure a good quality VLA inversion, the distances between the sound source and VLA are kept short (about 1 km).

In past years, geoacoustic data inversion for seabed properties using horizontal apertures (synthetic or towed arrays) has been proposed.[11,12] Jesus and Caiti[13] and Caiti, Jesus, and Kristensen[14] demonstrated the concept of MFP inversion with a towed array (156-m aperture) using narrowband data. Although broadband data were simulated, the measured data were only based on single frequencies. The feasibility test was successful, but several problems with the method are described in the concluding remarks of Ref. 14. Among the most important difficulties encountered were array shape deformation, low resolvability of the seabed parameters, and balancing the trade-off between computational efficiency and accuracy of the inversion solution. Each of these problem areas is addressed in this paper. Using a broadband signal transmission, the HLA shape is better estimated and the bottom properties are better resolved. Also, here, all geometric parameters (i.e., source and receiver positions and water depth) are included in the inversion process and do not rely completely on nonacoustic sensors. Using deeper tow depths for source and array together with a broadband signal received on a 254-m array provides a larger spread of reflection angles over a greater frequency band, and this additional information allows for an improved inversion. The inversions in this paper use a cost function (equivalent to a frequency-domain matched filter) that takes advantage of the broadband signal. The data inversions considered here use a set of seabed parameters that should minimize parameter coupling and allow for a more detailed description of the seabed than those in previous HLA inversions (i.e., sediment sound speed, layer thickness, attenuation, and sub-bottom sound speed are included). Finally, inversion of VLA measurements for exactly the same seabed parameters in the same location as for the HLA provides for a good comparison of the results.

In Sec. II of this paper the inversion procedure is described. In Sec. III, a simulation study is presented to illustrate and compare HLA and VLA geoacoustic inversion. A sensitivity study is presented to estimate which parameters might be resolved in the inversions. Section IV describes the

MAPEX2000 experiments and the acoustic data collected for validation of the inversion methods. Section V presents the geoacoustic inversion results using the MAPEX2000 experimental data taken on both a VLA and HLA.

II. INVERSION PROCEDURE

Measurements of acoustic data showing large differences in propagation loss for various locations around the world are indications that acoustics might be used in an inverse scheme to infer properties of the environment. This is the motivation for MFP, geoacoustic inversion. The method is summarized in the following list.

(1) Measure the acoustic field at the site of interest. A signal transmission covering a broad band of frequencies contains more information than that of a single tone and will generally produce better inversion results.[15] In the work considered in this paper, the band 220–800 Hz is considered. Although single hydrophone inversions are possible, arrays of receivers are generally more useful.

(2) Choose a propagation model that is suitable for the experimental conditions. For the HLA configuration considered here, the acoustic source is only a few hundred meters from the hydrophones. Steep angle propagation paths cannot be neglected and a model valid in the near-field must be used. Here, the broadband, complex normal-mode model ORCA[16] is used. This is a layered normal-mode model that includes the continuous spectrum. To demonstrate the robustness of the inversion approach, the parabolic equation method RAM[17] is also used as a propagation model. Other models may be appropriate, including ray theoretic codes that correctly treat the seabed interactions.

(3) Define a geoacoustic model for the site with a set of parameters that can be implemented in the propagation model. Only parameters which influence the down-range acoustic field should be considered. Otherwise, there is little hope that the acoustic fields will contain enough information to invert for those parameter values. Typically, a simplified description of the seabed is required to produce a stable inversion, as parameter coupling may cause an apparent instability.[18] Here, one- and two-sediment layer models overlying an infinite half-space are considered.

(4) Determine a cost function to quantify the agreement between the experimental measurements and the modeled data. Two cost functions based on the Bartlett correlator are used here.[19,20] The first correlates the modeled and measured pressure fields over the array of hydrophones and the magnitudes are summed over frequency as shown in Eq. (1)

$$B_H=\frac{1}{N_F}\sum_{j=1}^{N_F}\frac{|\Sigma_{i=1}^{N_H}p_{ij}q_{ij}^*|^2}{\Sigma_{i=1}^{N_H}|p_{ij}|^2\Sigma_{i=1}^{N_H}|q_{ij}|^2}. \tag{1}$$

The second cost function is given by Eq. (2). Here, the acoustic field is correlated in frequency with the magnitudes summed over the hydrophone array

$$B_F=\frac{1}{N_H}\sum_{i=1}^{N_H}\frac{|\Sigma_{j=1}^{N_F}p_{ij}q_{ij}^*|^2}{\Sigma_{j=1}^{N_F}|p_{ij}|^2\Sigma_{j=1}^{N_F}|q_{ij}|^2}. \tag{2}$$

In Eqs. (1) and (2), N_F is the number of frequency components, N_H is the number of hydrophones, and the measured and modeled complex pressure vectors are p_{ij} and q_{ij} (* denotes the complex conjugate operation). Both correlators take on a value of 1 for two identical signals and 0 for completely uncorrelated signals. Equation (1) is a maximum likelihood-derived objective function when the noise is additive and identically distributed on each hydrophone but the noise level may vary across frequencies. For Eq. (2), the noise is assumed identically distributed on each frequency but may vary across hydrophones. There were no obvious differences in the results for simulated data using either Eq. (1) or Eq. (2); however, with the experimental data Eq. (1) performed slightly better on the VLA and Eq. (2) slightly better on the HLA. The reason for this is not completely known, but it may be because the transmitted signal was better equalized to produce a flat spectrum [required for Eq. (2)] than the equalization to produce a flat hydrophone response across the HLA [required if using Eq. (1)]. For all inversions of measured data considered in this paper, Eq. (1) is used with the VLA and Eq. (2) with the HLA.

(5) An efficient algorithm is needed to navigate the enormous search space and find the global minimum to the cost function. This type of large-scale optimization requires a method such as genetic algorithms[4] or simulated annealing.[3] Both methods have been applied to MFP geoacoustic inversions with success. This is a constrained optimization problem with each of the desired inversion parameters bounded by a predetermined search space. In all the inversions considered in this paper (both HLA and VLA), a genetic algorithm search is used with the propagation models ORCA or RAM as implemented in the inversion code SAGA.[21] A total computation of 40 000 forward models was used in the inversion searches.

(6) Estimate the quality (errors) of the inversion. Several possibilities exist for estimating the accuracy of the inverted solution. A simple approach is to plot the cost function value versus corresponding parameter value. In this way, the distribution of high cost function values should cluster near the true parameter value. The character of such plots indicate the sensitivity of each parameter. This is shown with examples in Sec. III. Another important quality check is to examine the *a posteriori* distributions.[4]

A. Reducing the dominance of the direct and surface arrivals

The largest amplitude acoustic arrivals are usually due to the direct and sea-surface paths, yet these paths do not contribute to inversion for bottom properties. These arrivals depend only on the geometry of the experiment (i.e., source and receiver positions) and weakly on the ocean sound speed and sea-surface states. However, failure to account for these arrivals can significantly degrade the quality of the inversion results. One way to overcome allowing these arrivals from dominating the inversion problem would be to filter (or time gate) them. In practice, an automatic procedure to select from received time series only the surface and direct arrivals could be difficult. It can be especially complicated in cases

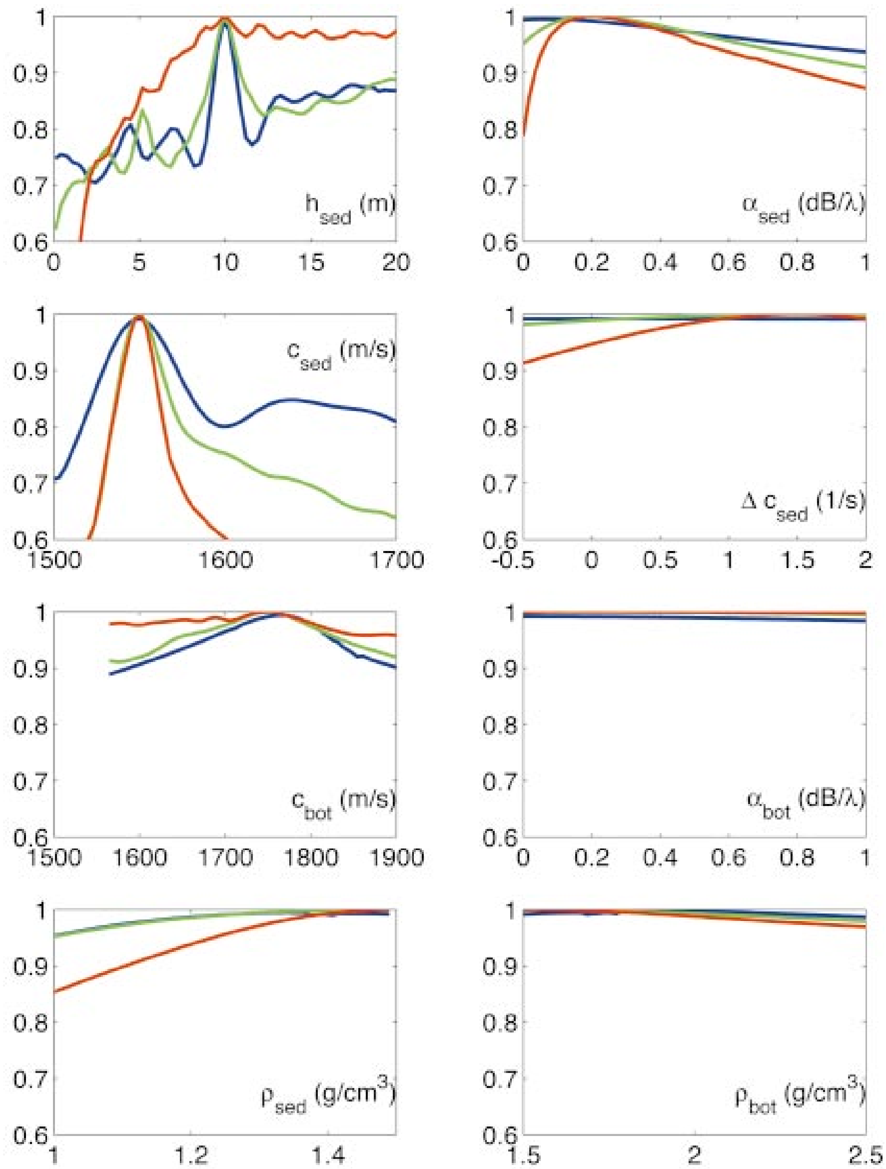

FIG. 4. Cost function evaluated against the reference solution as each seabed parameter takes on all its possible values. While evaluating a parameter, all of the others are held fixed at their known value. The cost function value is given on the *y*-axis and the parameter value on the *x*-axis. The blue curve gives the result for the horizontal array, the green curve for the vertical array moored 1 km from the source and the red curve is for a vertical array moored at 5 km. Reference and test solutions were simulated using ORCA.

when multiple arrivals interfere with each other (see Fig. 1). For instance, with a receiver and source at midwater depth the first surface and first bottom arriving paths will interfere. Nearly the same result as filtering can be accomplished by limiting the search intervals for geometric parameters. In principle, for geoacoustic inversion experiments, the geometry is known through direct measurements such as depth sensors on the towed source and receiver arrays. In practice, there is some slight uncertainty in source and receiver depths and other factors like array shape (e.g., tilt) may not be measured at all. There are also slight errors in the bottom depth measurement from the ship's echo sounder (on the order of 1 m for the MAPEX2000 experiments). Inverting acoustic measurements for source and receiver depths provides a valuable sanity check of the data quality and data processing. Furthermore, it avoids placing too much confidence in depth sensors and provides an estimate for array tilt.

Therefore, a two-step approach is used for the inversions considered in this paper. First, a geometry-only inversion is made, and second, these parameters are "locked down" for a full inversion for bottom properties. This is followed by a second inversion for geometric parameters only when using the newly inverted seabed parameters (as a check). This procedure is related to "focalization"[2] and the subspace approach of Refs. 22 and 23. For the measured data considered in Sec. IV, the geometry-only-inversion results agreed with the direct measurements (within experimental error). Additionally, the geometry-only inversion provided a valuable estimate for array tilt that was not readily available from direct measurements. Although the term locked down is used, the geometric parameters were not fixed at one value during the full inversion for bottom properties. The geometric parameters were allowed to vary by approximately the expected errors in the measurements. This approach is practical, since numerically the search for geometric parameters can be done extremely fast. Note the following normal-mode expression for the pressure field:

$$p(r,z)=\frac{\exp(i\pi/4)}{\rho(z_s)\sqrt{8\pi r}}\sum_{n=1}^{N}\frac{1}{\sqrt{k_{rn}}}\times\Psi_n(0,z_s)\Psi_n(r,z)\exp(ik_{rn}). \quad (3)$$

This assumes a time-harmonic $\exp(-i\omega t)$ point source in a cylindrical geometry positioned at range $r=0$ and depth $z=z_s$ with normal modes, $\Psi_n(z)$, corresponding horizontal wave numbers, k_{rn}, and density, $\rho(z)$.[24] The numerical approach is to compute the normal modes and horizontal wave numbers for one environment and store these in memory. Then, computing new pressure fields to invert for the geometry (i.e., source and receiver positions) requires only a repeat summation of Eq. (3) with new z_s, z, and r. The geometry-only inversion can be done in about 1% of the CPU time for a full inversion. By searching for these geometric parameters first, their search space can be greatly limited when included in the full inversion, which keeps the highly sensitive geometric parameters from dominating the inversion.

III. HORIZONTAL AND VERTICAL ARRAY SEABED CHARACTERIZATION: A SIMULATION STUDY

Much more research has been done using a VLA for matched-field geoacoustic inversion, and there is a good understanding of the sensitivity of both seabed parameters and experiment geometry. With the HLA, these sensitivities are less well known. A good initial discussion on HLA sensitivity can be found in Refs. 13 and 14. Some of the system and geometrical parameters that are expected to impact the inversion are as follows.

- (i) *Source and HLA depth*: It is expected that good insonification of the bottom favors towing closer to the seafloor. In practice, this can be difficult due to the danger of accidentally dragging the source or array on the bottom. Safe tow depths are usually determined based on how well the bathymetry of the area is known as well as how quickly equipment can be recovered.
- (ii) *Source and HLA separation*: It is also expected that better information will be obtained if the HLA receives from propagation directions around the critical angle. Since the critical angle is usually unknown, it may be difficult to set the ideal source–HLA separation distance.
- (iii) *Array length*: For a range-independent environment, longer HLAs should perform better than short ones (since more propagation angles would be received and therefore more information about bottom interactions). However, this has to be balanced by the practical issues such as array motion, more complicated propagation (over longer ranges), and possibly range dependence in the bathymetry or seabed properties.
- (iv) *Signal type and bandwidth*: Geoacoustic inversion using VLAs typically shows better performance using broadband rather than narrow-band signals. This is expected to be true also for HLA inversion.

In this section, using simulations, the sensitivity of seabed parameters determined with an HLA inversion method is compared with the sensitivity using a VLA. There are an enormous number of possible combinations of the aforementioned system and geometrical parameters; including all of them in this sensitivity study would confuse the results. Instead, these were fixed at the values used in the MAPEX2000 experiments described in Sec. IV.

TABLE I. Seabed parameters used to generate the reference solution. Parameter labels and search intervals are also shown. Attenuation and density are constant through the sediment and sub-bottom. Sound speeds refer to compressional acoustic waves and attenuation is given in units of decibels per wavelength.

Parameter	Reference value	Search minimum	Search maximum
Sediment thickness: h_{sed} (m)	10	0.1	20
Sediment speed: c_{sed} (m/s)	1550	1450	1700
Attenuation: α (dB/λ)	0.2	0.0	1.0
Density: ρ (g/cm^3)	1.5	1.0	2.5
Sub-bottom speed: c_{bot} (m/s)	1750	c_{sed}	$(c_{\mathrm{sed}}+250)$

Seabed sensitivity has a strong dependency on the parametrization used in the propagation modeling. Here, a one-layer geoacoustic model is used (sediment overlying a infinite half-space sub-bottom). Although this may seem overly simplistic, it is unlikely that a more highly resolved bottom could be extracted from these measurements and this inversion method.[9] Further, it is unlikely that a more sophisticated geoacoustic model would significantly change propagation predictions. This is explored further in Sec. V. Numerical simulations are used here to create a known set of data on both an HLA and VLA similar to the MAPEX2000 experimental data.

The first test of sensitivity is to look at each seabed parameter separately. For a selected parameter, the acoustic fields are computed for all values in its search space. Meanwhile, each of the other seabed parameters is held fixed at its known (reference) value. The eight parameters considered and their reference values are: sediment sound speed $c_{\mathrm{sed}}=1550$ m/s, sediment layer thickness $h_{\mathrm{sed}}=10$ m, sediment attenuation $\alpha_{\mathrm{sed}}=0.2$ dB/λ (wavelength), sediment density $\rho_{\mathrm{sed}}=1.5$ g/cm^3, sediment sound-speed gradient $\Delta c_{\mathrm{sed}}=1.5$ 1/s, sub-bottom sound speed $c_{\mathrm{bot}}=1750$ m/s, sub-bottom attenuation $\alpha_{\mathrm{bot}}=0.2$ dB/λ, sub-bottom density $\rho_{\mathrm{bot}}=1.5$ g/cm^3.

Three experimental geometries are considered: (1) HLA with the closest hydrophone 300 m away from the source; (2) VLA at 1-km source–receiver separation, and (3) VLA at 5-km separation. The water depth was taken as 130 m and the source depth was 55 m. The VLA had 48 hydrophones with 2-m spacing spanning the depths 24–118 m. The HLA was at 60 m depth, had 128 hydrophones with 2-m spacing spanning ranges 300–554 m from the source. The cost function was determined using Eq. (1) for both HLA and VLA,

TABLE II. Geometric parameters and search intervals around estimated values for geoacoustic inversions.

Parameter	Search interval
Source range	±5 m
Source depth	±1 m
Array depth	±1 m
Array tilt	±1 m
Bottom depth	±1 m

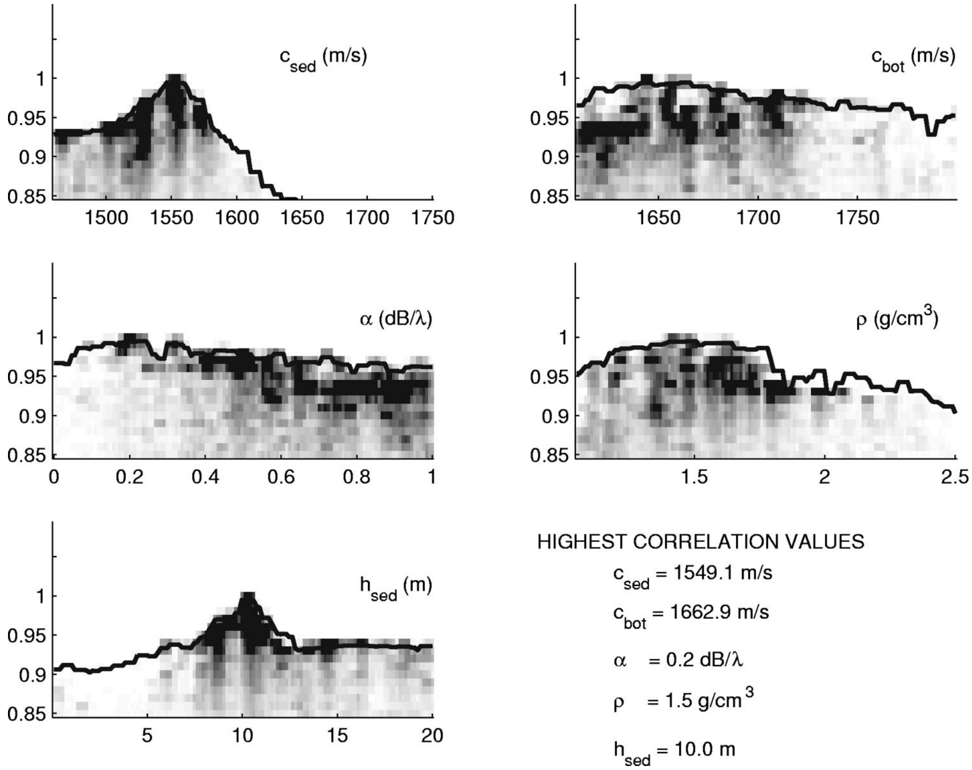

FIG. 5. Simulated data using ORCA: cost function values (along the *y*-axis without dimension) for the HLA at 300 m for each of 40,000 forward models included in the genetic algorithm search. Parameter and their units are indicated in the upper right corners of each panel and the *x*-axis corresponds to the search interval.

and the results for each parameter is given in Fig. 4. From Fig. 4, it can be seen that the VLA at 1 km and the HLA have the greatest sensitivity to h_{sed} and c_{bot}, while the VLA at 5 km is more sensitive to c_{sed} and ρ_{sed}. None of the geometries are sensitive to the sub-bottom attenuation (α_{bot}) or density (ρ_{bot}), and there is only slight sensitivity to sediment sound-speed gradient (Δc_{sed}). A caveat to this sensitivity test is the interdependency of each parameter on the others. For example, the sensitivity to sediment thickness and sub-bottom properties will also depend on the sediment properties (e.g., sound speed and density). That is, the ability to sense the sub-bottom and the interface between the sediment and sub-bottom will depend on the amount of penetration through the sediment. However, this simple sensitivity test provides both an estimate of how the cost function varies in the neighborhood of the true solution and guidelines for choosing param-

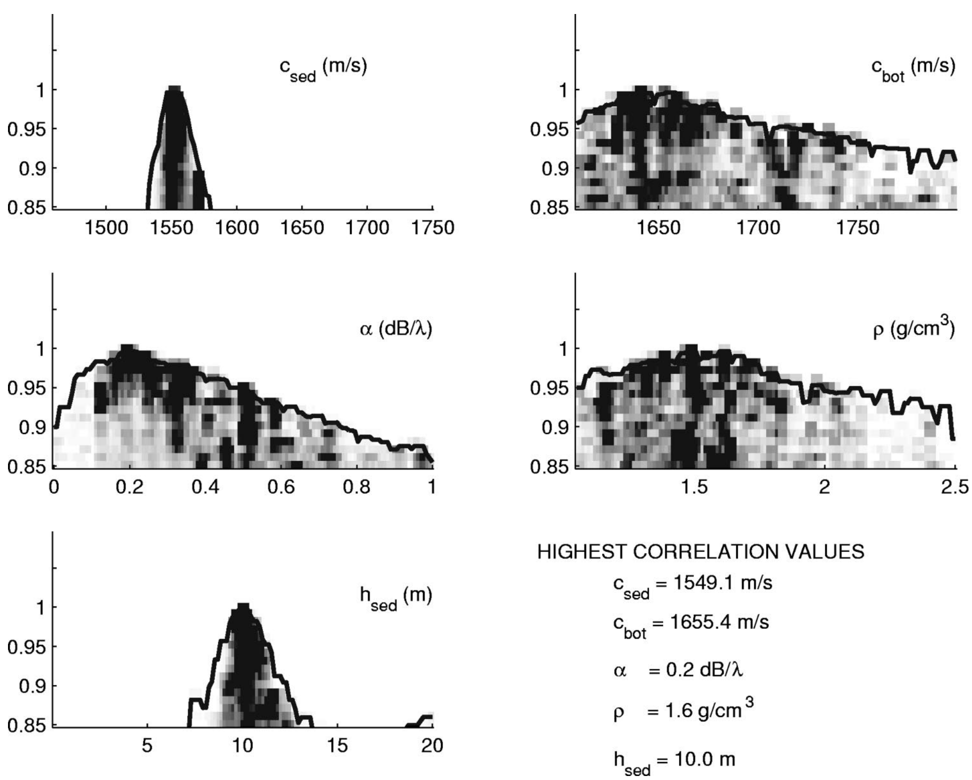

FIG. 6. Simulated data using ORCA: cost function values (along the *y*-axis without dimension) for the VLA at 1 km for each of 40,000 forward models included in the genetic algorithm search. Parameter and their units are indicated in the upper right corners of each panel and the *x*-axis corresponds to the search interval.

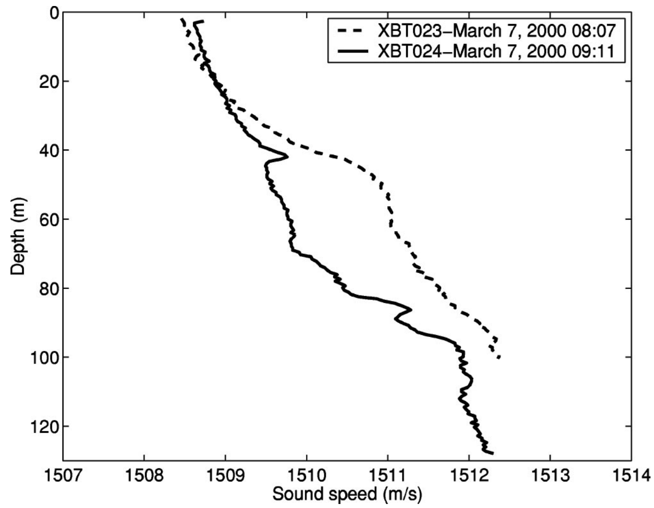

FIG. 7. Sound speed taken from XBT casts at positions 36°32.45′ N and 14°49.20′ E (at 8:07 UTC) 36°27.34′ N and 14°46.47′ E (at 9:11 UTC) on 7 March 2000.

eters. With the given sensitivity curves, the geoacoustic model was refined to include one sediment layer (over a half-space sub-bottom) but to ignore the sediment sound-speed gradient (e.g., constant sediment sound speed with depth) and to limit the model to a single attenuation and density (constant with depth through the sediment and sub-bottom).

A full inversion was performed on the reference solution using each of the three geometries described. The geoacoustic parameters for the simulation and the search intervals for the inversion are given in Table I. The geometrical parameters had small search intervals (the reasons for this are outlined in Sec. II A) and these are given in Table II.

The inversion results are presented in two ways. The set of parameter values corresponding to the single, highest correlation between reference and inverted solutions is given. Then, all the cost function values for each of the 40 000 forward model computations in the inversion are plotted with the corresponding parameter values. As the search algorithm converges, a particular part of the parameter space may be sampled more often than other parts. To give a sense of this sampling, a gray scale is used to indicate how the search algorithm sampled each parameter value. The most heavily sampled parts of the parameter search space appear darkest. These scatter plots reveal parameter sensitivity by showing how the cost function varies as the parameter search space is sampled. In this way, each parameter sensitivity can be judged without the bias imposed by keeping the other parameters fixed. The most likely value for each of the parameters can be interpreted from the peaks in the scatter plots. In Fig. 5 the scatter plot results from the HLA are shown, and in Fig. 6 the results from the VLA at 1 km. The scatter plots results resemble the sensitivity curves from Fig. 4. For both the VLA and HLA geometries, the scatter plots show heavy sampling and a peak at the correct value for each parameter. Figures 5 and 6 indicate higher sensitivity from the VLA, but the bottom properties are still resolved using the HLA.

IV. THE MAPEX2000 EXPERIMENTS

The MAPEX2000 experiments were conducted by the SACLANT Undersea Research Centre and took place on the Malta Plateau (between Italy and Malta) from 22 February to 27 March 2000. The purpose of the experiments described here is to validate the HLA geoacoustic inversion method and compare this with a VLA geoacoustic inversion. The

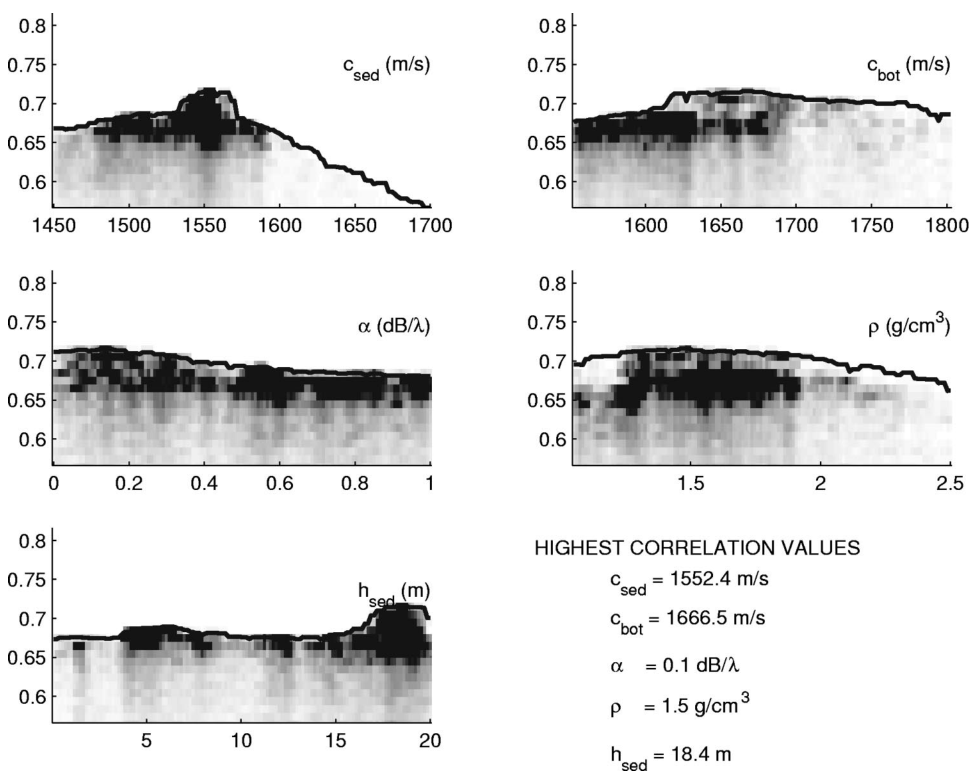

FIG. 8. MAPEX2000 HLA measured data inversion using propagation model ORCA from ping-9:07 on 7 March 2000. Cost function values (along the *y*-axis without dimension) for the HLA for each of 40,000 forward models included in the genetic algorithm search. Parameter and their units are indicated in the upper right corners of each panel and the *x*-axis corresponds to the search interval.

experimental setup showing the moored VLA and towed HLA is shown in Fig. 3. In this article, only the measurements taken on 7 March 2000 are considered.

A. Acoustic data

During the experiments of 7 March 2000, broadband acoustic signals were transmitted using flextensional sources mounted in a tow fish. A sequence consisting of linear frequency-modulated (LFM) sweeps and multitones were repeated every minute. In this paper, only 1-s sweeps from 150–800 Hz are considered. All transmissions were equalized using a programmable signal generator to produce signals having a flat spectrum. Prior to the 7 March 2000 experiments, the radiation patterns were measured from the sources showing no more than 1 dB directionality for the 150–800 Hz band.[25] Therefore, no correction was needed for the source radiation pattern (assumed omnidirectional). The received time series was converted to the frequency domain using a fast Fourier transform. Frequency bins corresponding to 220–800 Hz in 10-Hz increments were used in the inversion for comparison with modeled results.

The HLA is 254 m in total length, and for data considered here, the entire length of the array was used (128 hydrophones spaced at 2 m). Both the array and source were towed from the NRV ALLIANCE at approximately 5 knots. The distance between the sound source and the closest hydrophone on the HLA was about 300 m. The tow depth of the source and HLA varied slightly during the acoustic runs, but generally were maintained at 55–65-m depth. The VLA was deployed at position 36°26.668′ N and 14°46.751′ E and the acoustic data were received on NRV ALLIANCE by radio telemetry. The VLA has 48 equally spaced hydrophones covering 94 m of the water column (spanning depths of 24–118 m). The VLA was bottom moored (the water depth was 130 m) and kept upright using a subsurface float.

B. Oceanographic data

Sound-speed profiles were measured before, during, and after the acoustic experiments. Conductivity, temperature, and depth (CTD) measurements were taken from NRV ALLIANCE before and after each towed source acoustic run. During the acoustic runs, expendable bathythermograph (XBT) probes were deployed from NRV ALLIANCE to measure the ocean temperature profile. The salinity from the CTD casts were used to calculate sound speed from the XBT probes. Typical sound speeds taken from two XBT probes on 7 March 2000 are shown in Fig. 7. The profiles are slightly upward refracting (the typical condition for the experimental area in March), but the overall change in sound speed over depth is only about 4 m/s. For the two geoacoustic inversions considered here, the input sound-speed profile for the acoustic modeling was taken from the derived XBT closest in time to the acoustic transmission.

V. HORIZONTAL AND VERTICAL ARRAY SEABED CHARACTERIZATION: EXPERIMENTAL RESULTS

A 1-s LFM signal (150–800 Hz) was transmitted at 09:07 UTC from ALLIANCE located at 36°26.688′ N and 14°46.230′ E (denoted ping-9:07). This was simultaneously recorded on the HLA and the VLA (the VLA was about 1 km from the source). The same ping was inverted from receptions on the HLA and VLA with exactly the same procedure and search intervals as for the simulations in Sec. III. Equation (2) was used as the cost function for the HLA inversions and Eq. (1) for the VLA. The signal-to-noise ratio was about 20 dB for the data considered here. The scatter plots showing the most likely and highest correlation values for the seabed parameters are shown in Fig. 8 for the HLA and Fig. 9 for the VLA.

Both the HLA and VLA show clustering of the high cost-function values near the global maximum, best-fit solution, and both agree in the values for the seabed parameters that are most sensitive. Although the highest cost-function values (or fitness) are less than they were for the simulations, Figs. 8 and 9 have a 0.25 range on the cost-function axis (y axis) as was shown for the simulations Figs. 5 and 6. Since the signal-to-noise ratio was high, it is likely the lower overall cost function value was caused by a mismatch in the modeling of the experiment geometry, seabed, water column, or sea surface. As with the simulations, the VLA has slightly better sensitivity to the seabed parameters than does the HLA. However, clear values for the seabed parameters are found with the HLA in agreement with the VLA. Both HLA and VLA inversions indicate a dominant sediment layer at about 17–19-m depth.

A comparison of the measured and modeled (using ORCA) acoustic impulse responses are shown in Figs. 10 and 11. Both figures show multipath structure. For both the HLA and VLA, two of the first three strong arrivals contain no information about the seabed as these are direct and surface-bounce arrivals (the second arrival can be due to either the surface or the bottom bounce depending on geometry). Later arrivals have at least one interaction with the seabed. From Fig. 11, the tilt of the VLA can be inferred by the slight difference in direct path arrival times across the array. Using the arrival times along the array, and assuming the direct arrival is a plane wave, the VLA was tilted to give a 6–7-m displacement between the top and bottom hydrophones. Although this can be computed directly, it was left as an unknown and determined in the inversion process which found a value of 7-m VLA displacement (for the full inversion for bottom properties, the VLA tilt search interval was 6–8 m of displacement).

A. Geoacoustic inversion over a range-dependent seabed

The advantages of using a towed array–towed sound source configuration becomes clearer in range-dependent areas. For a fixed VLA like that used in MAPEX2000, only the sound source is mobile to probe the range-dependent environment. However, a VLA MFP inversion introduces modeling problems since the range-dependence needs to be included. The HLA configuration avoids this difficulty as the distance between source and receiver is kept small and range dependence can usually be neglected (slight range dependence such as water-depth changes can often be compensated for by allowing small shifts in source and receiver

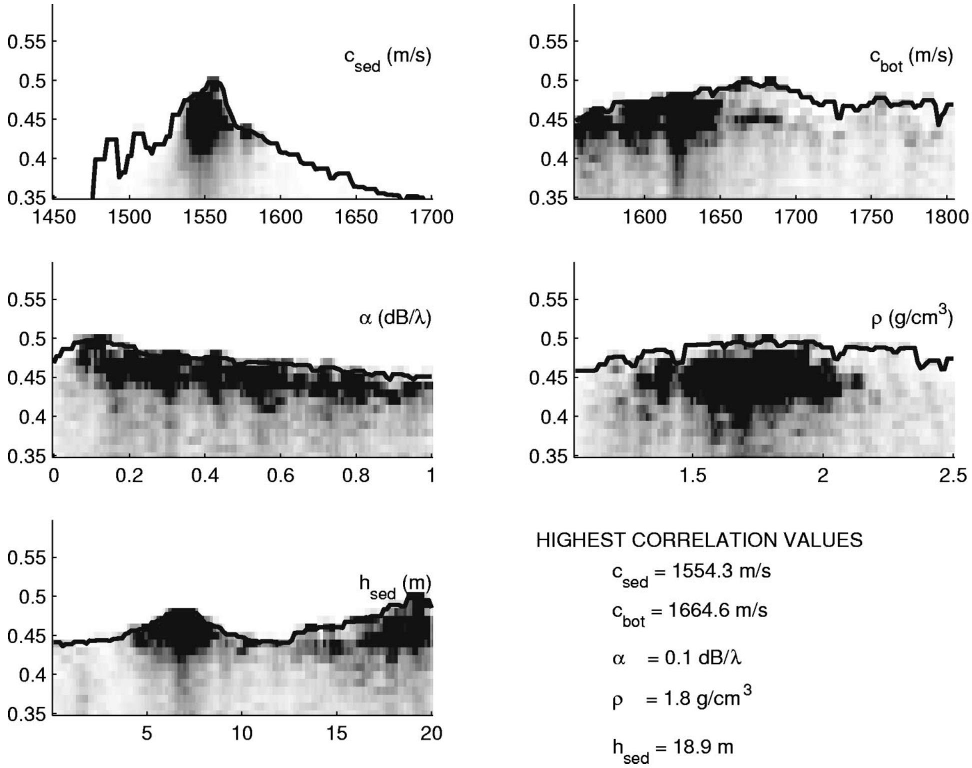

FIG. 9. MAPEX2000 VLA measured data inversion using propagation model ORCA from ping-9:07 on 7 March 2000. Cost function values (along the *y*-axis without dimension) for the VLA for each of 40,000 forward models included in the genetic algorithm search. Parameter and their units are indicated in the upper right corners of each panel and the *x*-axis corresponds to the search interval.

positions[26,27]). A second inversion was carried out for a ping taken at 08:05 UTC from ALLIANCE located at 36°32.580′ N and 14°49.260′ E (denoted ping-8:05). The water depth at the source–HLA location was 99 m and the VLA was still in the same position as for ping-9:07 (in water depth of 130 m). Doing a VLA inversion for ping-8:05 is problematic due only to the bathymetry change of 31 m between the source and VLA locations. Also, there is about 11 km between source and VLA, and range-dependent ocean sound speeds may need to be included. Further, the bottom properties also change along the track between ping-9:07 and ping-8:05. The area near ping-8:05 is characterized by a very soft layer on top of a harder sub-bottom. The HLA seabed inversion results are shown in Fig. 12. The different bottom type near

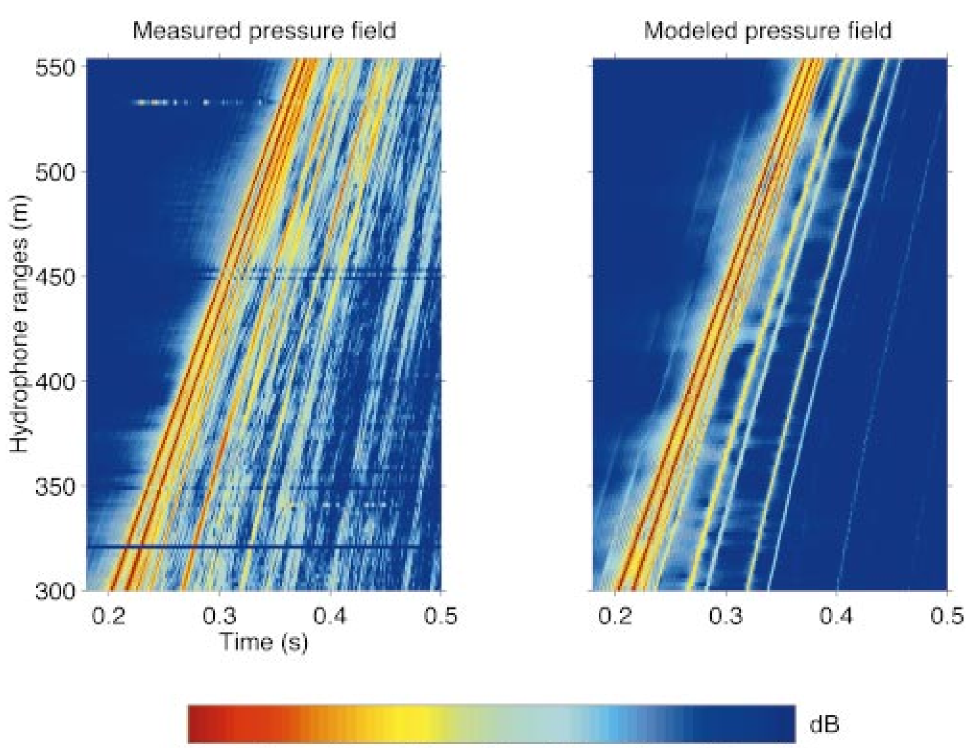

FIG. 10. Measured and modeled band-limited impulse responses for the HLA. The modeled field used the best fit seabed properties from the inversion.

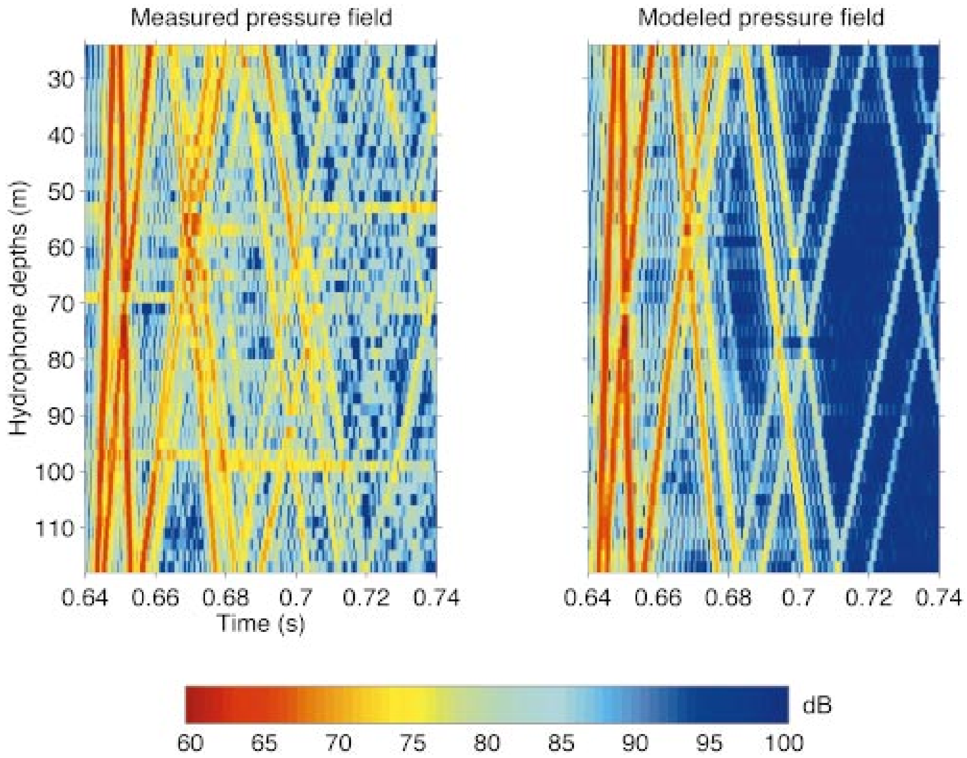

FIG. 11. Measured and modeled band-limited impulse responses for the VLA. The modeled field used the best fit seabed properties from the inversion.

ping-8:05 is evident from the results in Fig. 12. The soft layer is detected and is about 10 m in thickness. The lower sub-bottom speed is also well determined, which is likely because the soft sediment layer allows better acoustic penetration down to the sub-bottom. A VLA inversion was attempted using a range-independent assumption even though the water depth changed along the track by about 31 m. The VLA results showed a very poor cost-function value for the best-fit solution, and none of the geoacoustic parameters was well determined. It is possible that including the range-dependent bathymetry would improve the best-fit cost-function value; however, it would greatly increase computation time and it would remain difficult to interpret the averaged seabed properties found over the 11-km track.

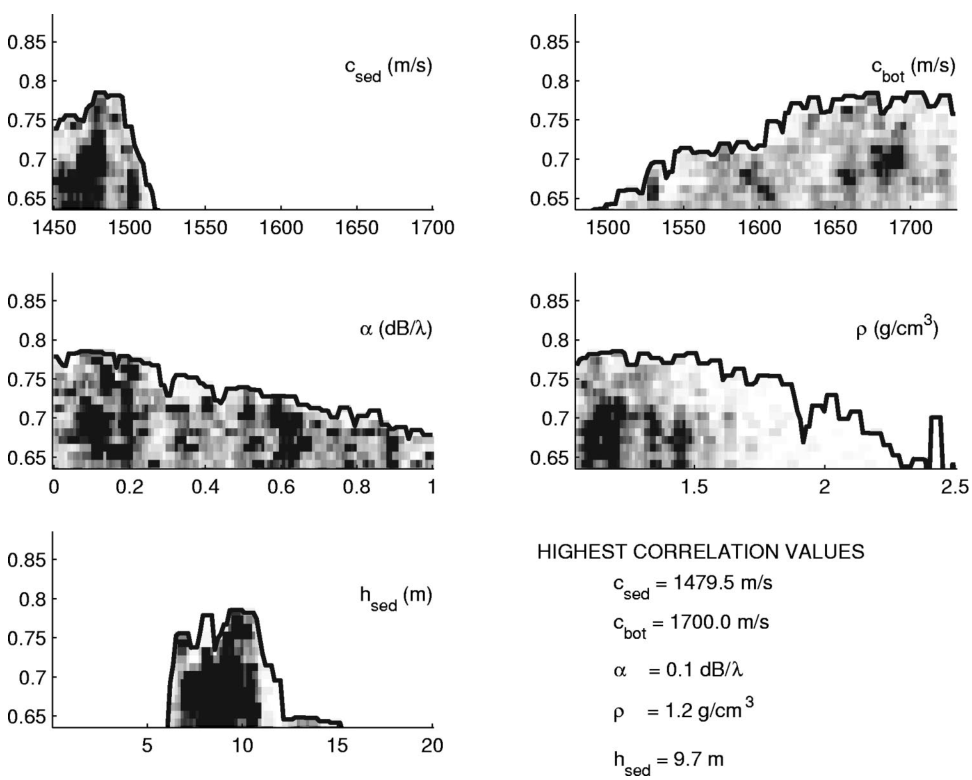

FIG. 12. MAPEX2000 HLA measured data inversion using propagation model ORCA from ping-8:05 on 7 March 2000. Cost function values (along the *y*-axis without dimension) for the HLA for each of 40,000 forward models included in the genetic algorithm search. Parameter and their units are indicated in the upper right corners of each panel and the *x*-axis corresponds to the search interval.

TABLE III. Geoacoustic properties for ping-8:05 using one-layer and two-layer models. Attenuation and density were assumed constant with depth through the sediment.

Parameter	One-layer model	Two-layer model
Sediment-1 thickness: h_{sed1} (m)	9.7	9.3
Sediment-2 thickness: h_{sed2} (m)	⋯	9.5
Sediment-1 speed: c_{sed1} (m/s)	1480	1487
Sediment-2 speed: c_{sed1} (m/s)	⋯	1695
Sub-bottom speed: c_{bot} (m/s)	1700	1763
Attenuation: α (dB/λ)	0.1	0.01
Density: ρ (g/cm^3)	1.2	1.4

A second inversion was made on ping-8:05 using a more sophisticated geoacoustic model that included two sediment layers over an infinite half-space. Within each of the two layers the geoacoustic properties were assumed constant (no gradients). As an additional check, the forward propagation model RAM was used in place of ORCA. The search algorithm and objective function are the same as those already described. The results of the comparison are shown in Table III. The table shows the two inversions produce a similar seabed. The slow layer of about 9–10 m over a faster layer is again well determined. The second layer of the two-layer model has a sound speed nearly the same as the half-space of the one-layer model. Both inversions produce low attenuation and a similar density. The significance of the one-layer and two-layer inversions demonstrates that for these data the method is not particularly sensitive to the propagation model, and that the one-layer model is probably adequate to describe the seabed.

Inversion of the data taken between ping-8:05 and ping-9:07 is useful to show how the inverted seabed properties vary along the track. Inversion results for nine pings along the track, using the two-layer geoacoustic model with propagation model RAM, are shown in Fig. 13. The figure shows the inverted sound speed in the seabed and the inverted layering. As previously noted, for ping-8:05 the two-layer RAM inversion results are very similar to the one-layer ORCA results and the same is true for ping-9:07. For ping-9:07, the two-layer model results indicate nearly the same properties in both layers ($c_{sed1}=1550$ m/s and $c_{sed2}=1563$ m/s), which implies the existence of only one dominant sediment layer. The average speed in both layers of 1557 m/s and combined layer thickness of 19.8 m agrees well with the one-layer ORCA results, giving speed of 1554 m/s and thickness of 18.9 m. There is also a consistency between pings taken near each other (in time and space), and there was a fairly gradual change in the inverted seabed properties moving along the range-dependent track. The slow sediment layer (sound speed less than that in the water column) that was evident from ping-8:05 was apparent in other pings along the track, but this layer gradually became thicker, moving along the track from ping-9:07 to ping-8:05 (Fig. 13).

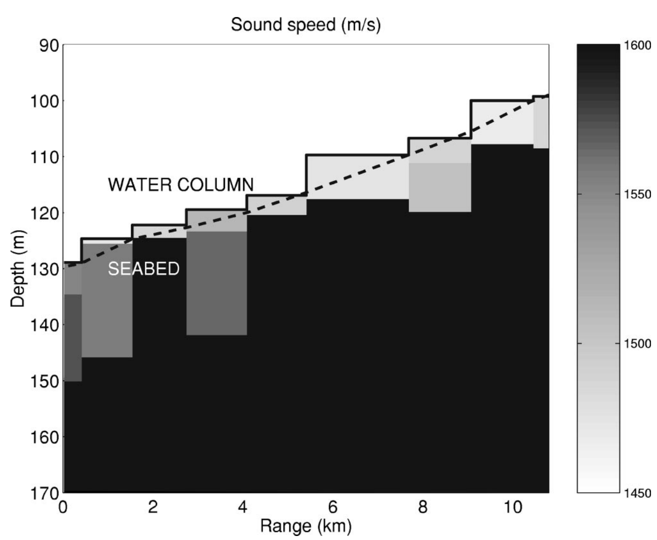

FIG. 13. MAPEX2000 HLA measured data inversion between sites 1 (ping-9:07) and 4 (ping-8:05) on 7 March 2000 using 2-layer geo-acoustic model and propagation model RAM. Layer thickness and sound speed in the sediment are shown. Inverted properties are held constant in range between data points. Solid lines (stair-steps) are indicated at inverted water depth values and measured bathymetry is given by the dashed line.

VI. CONCLUSIONS

Knowing the geoacoustic properties of the seabed is critical for accurate acoustic propagation modeling for sonar performance prediction. This paper describes an inversion method to obtain these geoacoustic parameters using a towed horizontal line array (HLA) of receivers and a broadband sound source. Matched-field processing (MFP) geoacoustic inversion methods have been shown as a promising technique for determining seabed properties, but most of the research has used measurements from a vertical line array (VLA). A towed array has many advantages over the moored, vertical array configuration such as easier deployments and being able to neglect range dependence in the MFP inversion while still mapping range-dependent seabed properties.

An important validation for the HLA inversions presented here is the comparison with the VLA inversion, and results are in good agreement for data taken where the source was near the VLA (where it is expected the VLA inversion will perform best). For an 11-km track the VLA data inversion did not perform well due to the range-dependent environment. Using the HLA data inversion this problem was circumvented, making it possible to determine seabed properties along the entire 11-km track. In this sense, the HLA inversions outperformed the VLA inversions.

Several issues need to be addressed in future research and three main ones are listed here. (1) *Computational*—The computational demands using normal-mode or parabolic equation forward models are still quite high and for practical, real-time seabed estimates a propagation code will be required that is fast, includes all the physics of the seabed interactions, and is valid near the sound source. Ray tracers may offer a good alternative to normal modes or parabolic equation methods for rapidly computing broadband impulse responses. It may be possible to use a ray tracer if the acoustic bottom interactions are treated correctly.[28,29] (2) *Geometry*—The ideal measurement geometry will also need to be determined as it is likely that parameters like array length, tow depths, and signal types will need to be optimized to improve estimates of the seabed properties. (3) *Cost functions*—Cost functions have different sensitivities that depend on array type, signal type, and seabed parameterization. There may be a better set of cost functions (than used here) to improve the performance of HLA inversions.

ACKNOWLEDGMENTS

The authors wish to acknowledge all the members who participated in MAPEX2000. Special thanks to E. Michelozzi as engineering coordinator and P. Boni for managing the data acquisition of data. The authors would also like to gratefully acknowledge the crews of NRV ALLIANCE and ITNS TAVOLARA.

[1] R. J. Urick, *Sound Propagation in the Sea* (Defense Advanced Research Projects Agency, Washington, D.C., 1979).

[2] M. D. Collins and W. A. Kuperman, ''Focalization: Environmental focusing and source localization,'' J. Acoust. Soc. Am. **90**, 1410–1422 (1991).

[3] M. D. Collins, W. A. Kuperman, and H. Schmidt, ''Nonlinear inversion for ocean bottom properties,'' J. Acoust. Soc. Am. **92**, 2770–2783 (1992).

[4] P. Gerstoft, ''Inversion of seismo-acoustic data using genetic algorithms and *a posteriori* probability distributions,'' J. Acoust. Soc. Am. **95**, 770–782 (1994).

[5] D. F. Gingras and P. Gerstoft, ''Inversion for geometric and geoacoustic parameters in shallow water: Experimental results,'' J. Acoust. Soc. Am. **97**, 3589–3598 (1995).

[6] J. P. Hermand and P. Gerstoft, ''Inversion of broadband multi-tone acoustic data from the Yellow Shark summer experiments,'' IEEE J. Ocean. Eng. **21**, No. 4, 324–346 (1996).

[7] N. R. Chapman and A. Tolstoy, ''Special issue: Benchmarking geoacoustic inversion methods,'' J. Comput. Acoust. **6**, No. 1&2, 1–289 (1998).

[8] M. Siderius, M. Snellen, D. Simons, and R. Onken, ''An environmental assessment in the Strait of Sicily: Measurement and analysis techniques for determining bottom and oceanographic properties,'' IEEE J. Ocean. Eng. **25**, No. 3, 364–386 (2000).

[9] M. Siderius, P. Nielsen, J. Sellschopp, M. Snellen, and D. Simons, ''Experimental study of geoacoustic inversion uncertainty due to ocean sound-speed fluctuations,'' J. Acoust. Soc. Am. **110**, 769–781 (2001).

[10] C. Holland and J. Osler, ''High-resolution geoacoustic inversion in shallow water: A joint time- and frequency-domain technique,'' J. Acoust. Soc. Am. **107**, 1263–1279 (2000).

[11] G. V. Frisk and J. F. Lynch, ''Shallow water waveguide characterization using the Hankel transform,'' J. Acoust. Soc. Am. **76**, 205–216 (1984).

[12] W. A. Kuperman, M. F. Werby, K. E. Gilbert, and G. J. Tango, ''Beam forming on bottom-interacting tow-ship noise,'' IEEE J. Ocean. Eng. **10**, No. 3, 290–298 (1985).

[13] S. M. Jesus and A. Caiti, ''Estimating geoacoustic bottom properties from towed array data,'' J. Comput. Acoust. **4**, No. 3, 273–290 (1996).

[14] A. Caiti, S. M. Jesus, and A. Kristensen, ''Geoacoustic seafloor exploration with a towed array in a shallow water area of the Strait of Sicily,'' IEEE J. Ocean. Eng. **21**, No. 4, 355–366 (1996).

[15] G. Haralabus and P. Gerstoft, ''Source localization in shallow water using multi-frequency processing of shot data,'' Technical Report SR-253, SACLANT Undersea Research Centre, La Spezia, Italy, 1996.

[16] E. K. Westwood, C. T. Tindle, and N. R. Chapman, ''A normal mode model for acousto-elastic ocean environments,'' J. Acoust. Soc. Am. **100**, 3631–3645 (1996).

[17] M. D. Collins, ''A split-step Padé solution for parabolic equation method,'' J. Acoust. Soc. Am. **93**, 1736–1742 (1993).

[18] M. Snellen, D. Simons, M. Siderius, J. Sellschopp, and P. Nielsen, ''An evaluation of the accuracy of shallow-water matched-field inversion results,'' J. Acoust. Soc. Am. **109**, 514–527 (2001).

[19] P. Gerstoft and C. F. Mecklenbräuker, ''Ocean acoustic inversion with estimation of *a posteriori* probability distributions,'' J. Acoust. Soc. Am. **104**, 808–819 (1998).

[20] C. F. Mecklenbräuker and P. Gerstoft, ''Objective functions for ocean acoustic inversions derived by likelihood methods,'' J. Comput. Acoust. **8**, 259–270 (2000).

[21] P. Gerstoft, ''SAGA Users Manual 2.0, an inversion software package,'' Technical Report SM-333, SACLANT Undersea Research Centre, La Spezia, Italy, 1997.

[22] P. Ratilal, P. Gerstoft, and J. T. Goh, ''Subspace approach to inversion by genetic algorithms involving multiple frequencies,'' J. Comput. Acoust. **6**, No. 1&2, 99–115 (1998).

[23] M. I. Taroudakis and M. G. Markaki, ''Bottom geoacoustic inversion by matched-field processing—A sensitivity study,'' Inverse Probl. **16**, 1679–1692 (2000).

[24] F. B. Jensen, W. A. Kuperman, M. B. Porter, and Henrik Schmidt, *Computational Ocean Acoustics* (American Institute of Physics, New York, 1994).

[25] L. Troiano, ''Sound source for MAPEX2000,'' Internal memorandum to M. Siderius on sound source calibration for MAPEX2000 experiments, 22 February 2000.

[26] G. L. D'Spain, J. J. Murray, W. S. Hodgkiss, N. O. Booth, and P. W. Schey, ''Mirages in shallow-water matched-field processing,'' J. Acoust. Soc. Am. **105**, 3245–3265 (1999).

[27] C. H. Harrison and M. Siderius, ''Correlations between search parameters in geoacoustic inversion,'' in *Proceedings of the Fifth European Conference on Underwater Acoustics* [European Commission, Rue de la Loi/Wetstraat 200 (SDME 7/85), B-1049 Brussels, 2000], pp. 203–208, Directorate-General for Research.

[28] E. K. Westwood and P. J. Vidmar, ''Eigenray finding and time series simulation in a layered-bottom ocean,'' J. Acoust. Soc. Am. **81**, 912–924 (1987).

[29] E. K. Westwood and C. T. Tindle, ''Shallow-water time series simulation using ray theory,'' J. Acoust. Soc. Am. **81**, 1752–1761 (1987).